STScI | SPACE TELESCOPE SCIENCE INSTITUTE

JWST TECHNICAL REPORT

Title: The Early Behavior of the NIRISS Pupil Wheel and Filter Wheel	Doc #: JWST-STScI-008298, SM-12 Date: 1 November 2022 Rev: -
Authors: André R. Martel Phone: 410-338-4888	Release Date: 15 December 2022

1 Abstract

The quality and consistency of the images and spectra collected by NIRISS are highly dependent on the behavior of its Pupil Wheel (PW) and Filter Wheel (FW). Here, we analyze the basic telemetry of the wheels over the first ten months of on-orbit activities to establish a baseline of their behavior for future monitoring and trending. This period includes the six-month commissioning campaign and the early part of Cycle 1, including the Early Release Observations (ERO) and Early Release Science (ERS) programs as well as some Guaranteed Time Observations (GTO) and General Observers (GO) programs. We find that the total usage of the wheels is currently well below the on-orbit allocations and their positional accuracy is within the expected range of ± 1 motor step but with some possible trends on their direction of motion. In some sequences of consecutive exposures in the same wheel element, the wheel sometimes moves slightly between exposures, possibly leading to different tilts in the grism spectra. The voltages of the Variable Reluctance (VR) sensor of both wheels are as expected for all the wheel elements.

2 Introduction

The PW and FW of NIRISS are Limited Lifetime Items (LLI) that house all the imaging and spectral elements of the four science modes of this instrument. These elements are the GR700XD grism for the Single Object Slitless Spectroscopy (SOSS) mode, the Non-Redundant Mask (NRM) for the Aperture Masking Interferometry (AMI) mode, the GR150C and GR150R grisms for the Wide Field Slitless Spectroscopy (WFSS) mode, and the medium- and broad-band imaging filters for the Imaging mode (Fig. 2-1). A failure of one or both wheels, also known as the Dual Wheel (DW), would be catastrophic to the scientific productivity of NIRISS. It is therefore crucial to understand the behavior of the DW early in the mission and establish a baseline of its relevant telemetry for long-term trending and to help identify any future degradation of its performance.

In the following, we present the telemetry that is the most relevant for monitoring the long-term health of the DW: the behavior and accuracy of the position of the wheel elements and the voltage of the Variable Reluctance (VR) sensors. We also provide an update of the usage of the wheels at the time of writing of this report.

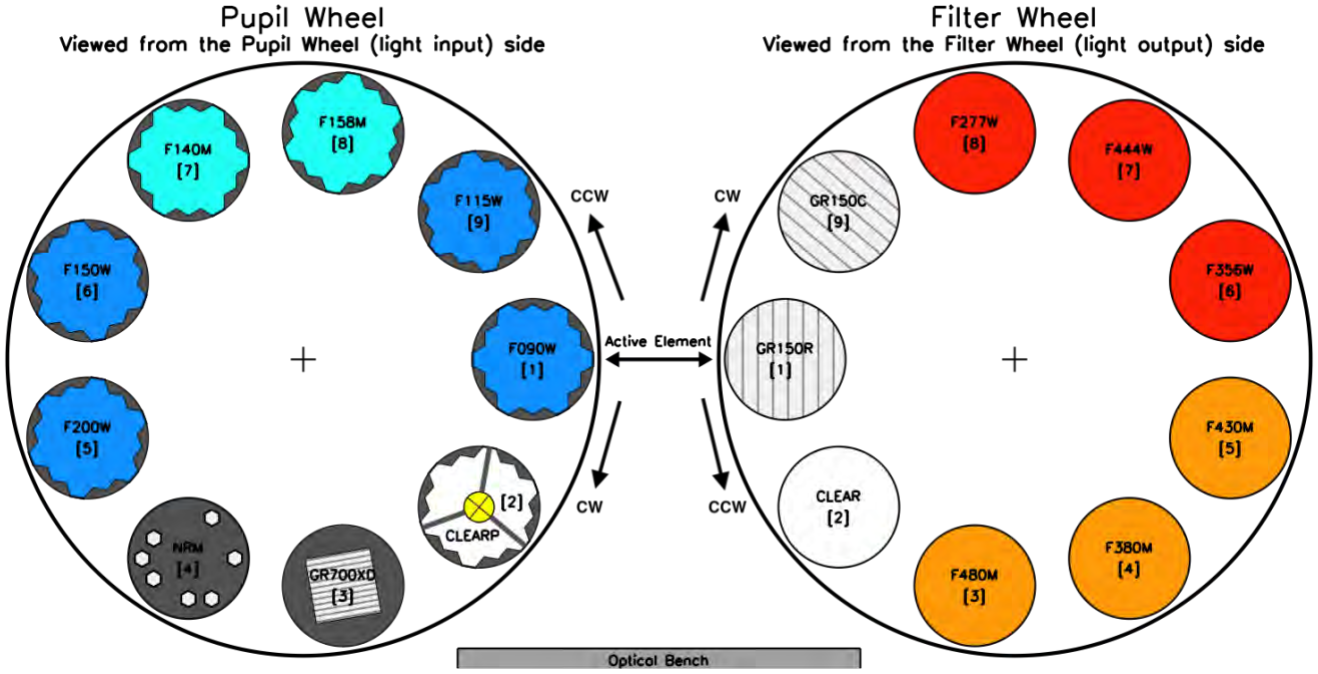

Figure 2-1. Schematic of the NIRISS DW. In the light path of NIRISS, a photon traverses the PW before the FW.

3 Telemetry

The values of the basic telemetry mnemonics of the DW were extracted with the Web Offline Workspace (WOW) system on the Flight Operations Subsystem (FOS) at STScI. The data span the on-orbit lifetime of NIRISS up to this point, from the power-on and initialization on Jan 28, 2022 to Nov 28, 2022. This period includes the entire six-month commissioning campaign and approximately four months of Cycle 1 observations. The telemetry of ten mnemonics was extracted at the highest sampling rate of ≈ 4 sec for each wheel, resulting in a large text file (1.4 Gb) that was manipulated with Python scripts to generate plots and statistics. For the purposes of this report, we only consider the telemetry mnemonics listed in Table 3-1. The INIS_PWC_PUPIL and INIS_FWC_FILTER mnemonics indicate the name of the active element of the wheel, INIS_PWC_POS and INIS_FWC_POS give the position of the wheel in degrees, INIS_PWC_MOV and INIS_FWC_MOV indicate the direction of the last movement of the wheel, either clockwise (CW) or counter clockwise (CCW) (see Fig. 2-1), and INIS_PWVRVOL and INIS_FWVRVOL give the voltage of the VR sensor.

Table 3-1. DW Telemetry

Mnemonic	Description
INIS_PWC_PUPIL	Current PW element
INIS_PWC_POS	Position of PW element (°)
INIS_PWC_MOV	Direction of last movement of the PW
INIS_PWVRVOL	VR sensor voltage of the PW (Volt)
INIS_FWC_FILTER	Current FW element
INIS_FWC_POS	Position of FW element (°)
INIS_FWC_MOV	Direction of last movement of the FW
INIS_FWVRVOL	VR sensor voltage of the FW (Volt)

The center positions of the elements of the PW and FW, as commanded by the Flight Software (FSW), are part of the INIS_DWC_PUPIL_POS_TBL (6110) and INIS_DWC_FILTER_POS_TBL (6111) tables of the Flight Operations (OPSFLT) partition of the JWST Project Reference Database (PRD). They are also tabulated in Martel (2020) and for easy reference are listed in Tables 3-2 and 3-3 below. The accuracy of the position of the active element of each wheel is ± 1 motor step, which corresponds to $\pm 0.1651°$ and $\pm 0.1585°$ at the PW and FW, respectively (Delamer et al. 2015). The position of the wheel elements is therefore not repeatable, i.e., we expect a range of positions about the expected center position. Although small, these angles can translate to tilts of a few pixels over the full length of the SOSS and WFSS spectral traces and degrade the reliability of the fringes for the AMI mode.

Table 3-2. PW Center Positions

Position	Name	Resolver Reading (Wheel Degrees) $\pm\, \mathbf{0.1651}°$
1	F090W	325.0131
2	CLEARP	284.9032
3	GR700XD	245.7600
4	NRM	204.9813
5	F200W	164.8715
6	F150W	124.9032
7	F140M	84.9007
8	F158M	44.9374
9	F115W	4.9789

Table 3-3. FW Center Positions

Position	Name	Resolver Reading (Wheel Degrees) $\pm 0.1585°$
1	GR150R	33.5667
2	CLEAR	74.8667
3	F480M	114.9667
4	F380M	154.8889
5	F430M	194.8111
6	F356W	234.9333
7	F444W	274.9000
8	F277W	314.8667
9	GR150C	354.2111

The voltage of the VR sensor indicates when the wheel is at position 1 (F090W for the PW and GR150R for the FW). At this position, the sensor is triggered and its voltage shows a higher value than at the other wheel positions. The range of the voltages measured in the OTIS cryo test campaign at the Johnson Space Center (JSC) (Jul – Oct 2017) (Martel 2021a, b) is listed in Table 3-4. Typically, the voltage at position is about 1.7 Volts greater than at the other positions. It's important to note that the FSW does not rely on the voltage to track the position of the wheels; it is simply extra, easy to understand information that shows the absolute position of the PW. It can be useful, for example, if the position of the wheel is lost – one could simply command a full revolution of the wheel and note when the voltage spikes to locate position 1. But over time, the VR sensor voltage may drift outside the detection range of the FSW and will therefore need to be recalibrated. Typically, this will be required when the difference in voltage between position 1 and the neighboring positions is $\lesssim 1$ Volt. The recalibration is an iterative and complicated process and is described in detail in the contingency Commissioning Activity Requests (CARs) NIS-025-C (PW) and NIS-026-C (FW). In this report, we simply monitor the voltages to verify their long-term stability and determine if a recalibration is required.

Table 3-4. VR Sensor Voltages in the OTIS Ground Cryo Campaign

Mnemonic	Value (Volt)
INIS_PWVRVOL	Position 1 (F090W): 4.16 – 4.25
	Other positions: 2.35 – 2.39
INIS_FWVRVOL	Position 1 (GR150R): 3.67 – 3.76
	Other positions: 2.13 – 2.14

4 Results

In the following, we summarize the usage of the PW and FW so far in the JWST mission and discuss the accuracy of the wheel positions as well as the behavior of the wheels in consecutive exposures in the same wheel element.

4.1 Usage

The PW and FW wheel motors were designed to meet the science requirements of NIRISS for a 0.5-year commissioning campaign followed by a five-year mission. The on-orbit and lifetime allocations of the DW usage are based on early science scenarios that assumed NIRISS would account for 10% of the total Observatory time. The rationale and details of the allocations are presented in Vila Costas (2015) and references therein – we will not repeat them here. In Table 4-1, we list the number of steps and rotations of both wheels in the commissioning programs (Martel et al. 2022) and in the Cycle 1 programs as of Nov 28, 2022, as well as the on-orbit allocations for 5.5 years. The usage of the PW and FW represents about 9% and 20% of their on-orbit allocations so far. Similarly, in Table 4-2, we include the wheel usage in the ground cryo campaigns as tabulated by the Limited Life Tracking Tool of W. Baggett (STScI). The lifetime allocations at cryo temperatures, excluding any margins, are also tabulated. The lifetime usage as of Nov 28, 2022 amounts to about 23% and 38% of the allocations for the PW and FW, respectively. But we note that the lifetime allocation of the FW has a margin of 23834 steps (2648 rotations). If we include these additional steps or rotations in our tally, then the lifetime usage of the FW is about 10% so far.

These usages are already significant after only four months of Cycle 1 operations. We therefore predict that the total usage of the wheel mechanisms will exceed the on-orbit and lifetime allocations over a period of 5.5 years. We note that the NIRISS GO and GTO programs represent approximately 8.5% of the Observatory time in Cycle 1, slightly smaller than the assumed value of 10% (but likely closer if the calibration programs are considered). Moreover, in future cycles, imaging will be offered as a prime observing mode, thus increasing the wheel usage further.

Table 4-1. PW and FW On-Orbit Usage (as of Nov 28, 2022)

	PW		FW	
	Steps	**Rotations**	**Steps**	**Rotations**
Commissioning	454	50.4	621	69.0
Cycle 1	476	52.9	649	72.1
Total On-Orbit Usage	930	103	1270	141
Total On-orbit Allocation	9927	1103	6471	719
% of On-orbit Allocation	9.4%		19.6%	

Note: One 360° rotation of a wheel consists of nine steps.

Table 4-2. PW and FW Lifetime Usage (as of Nov 28, 2022)

	PW		FW	
	Steps	**Rotations**	**Steps**	**Rotations**
Ground Cryo	1779	198	1884	209

	PW		FW	
	Steps	**Rotations**	**Steps**	**Rotations**
Commissioning	454	50.4	621	69.0
Cycle 1	476	52.9	649	72.1
Total Lifetime Usage	2709	301	3154	350
Total Lifetime Allocation	11619	1291	8305	923
% of Lifetime Usage	23%		38%	

Note: One 360° rotation of a wheel consists of nine steps.

4.2 Offsets from the Center Positions

We verify the accuracy and repeatability of the PW and FW positions by comparing their observed and expected center values.

4.2.1 Pupil Wheel

In Fig. 4-1, we plot the distribution of the unique absolute positions (in degrees) of the nine elements of the PW. The distribution is red when the element settles in the light path from the CW direction and blue when approaching from the CCW direction. Consecutive exposures in the same wheel element can sometimes show slightly different positions (see Section 4.3) – these are included in the histograms. Although the usage of any given PW element is small, we find that the PW is well behaved – all the positions are within the range of ± 1 motor step (green vertical solid lines) and generally centered on their expected positions (dashed vertical black line). For more robust statistics, the offsets between the observed and expected center positions for all the wheel elements are combined into a single histogram in Fig. 4-2. Normal distributions are fit to the core ($\pm 1/2$ motor step) as approximations. The histograms of the offsets are clearly asymmetrical and do not peak at the commanded positions. In particular, the CW histogram shows an excess at offsets less than about $-0.05°$ while the CCW has an excess at offsets greater than about $0.10°$. Hence the final position of a PW element is not exactly centered on the expected position but appears biased depending on the direction of motion of the wheel.

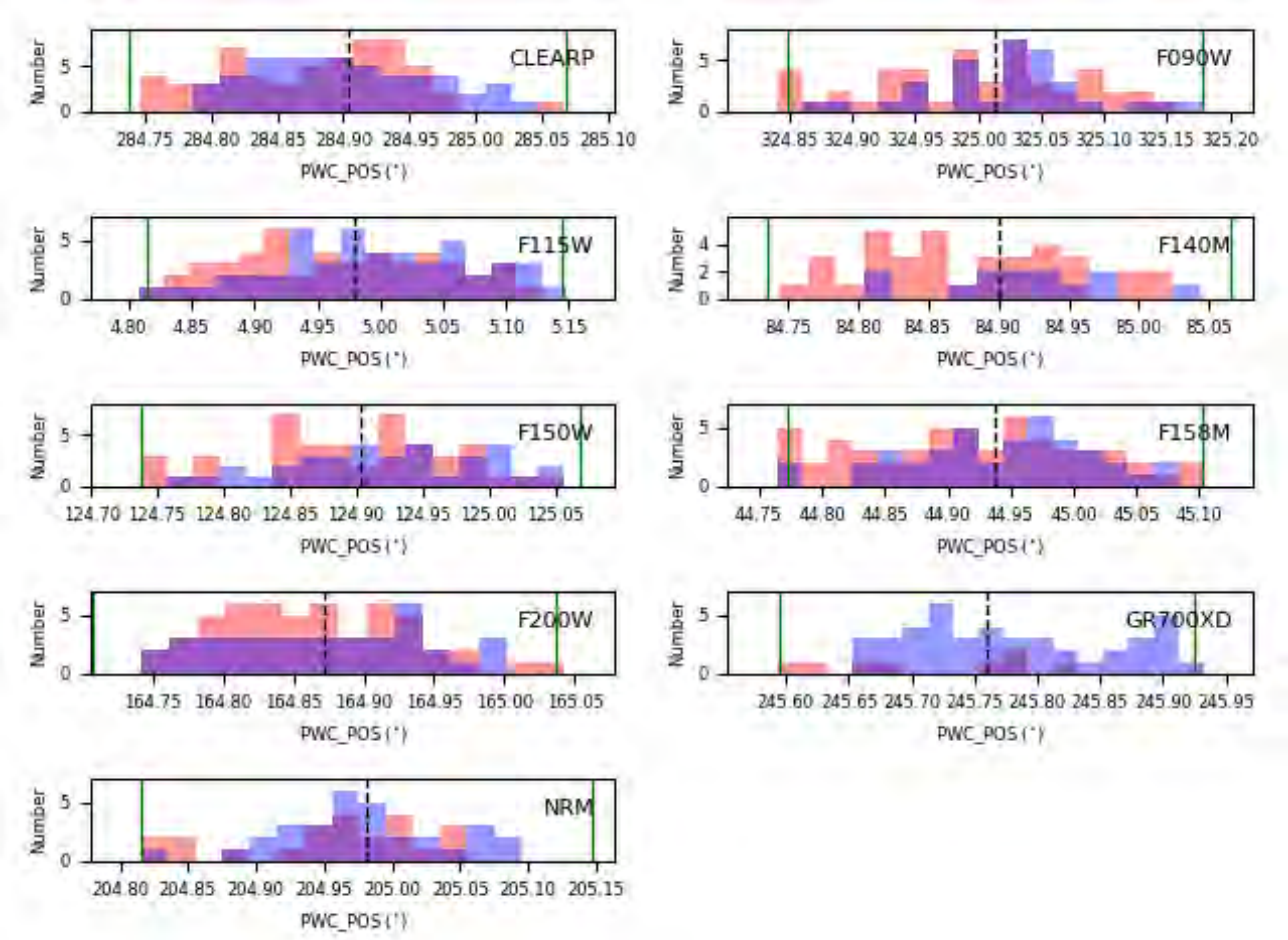

Figure 4-1. The distribution of the observed position of each PW element in wheel degrees (PWC_POS) is shown. The vertical dashed line denotes the expected center position and the green lines the uncertainty of one motor step ($\pm 0.1651°$). The CW rotations are in red and CCW in blue.

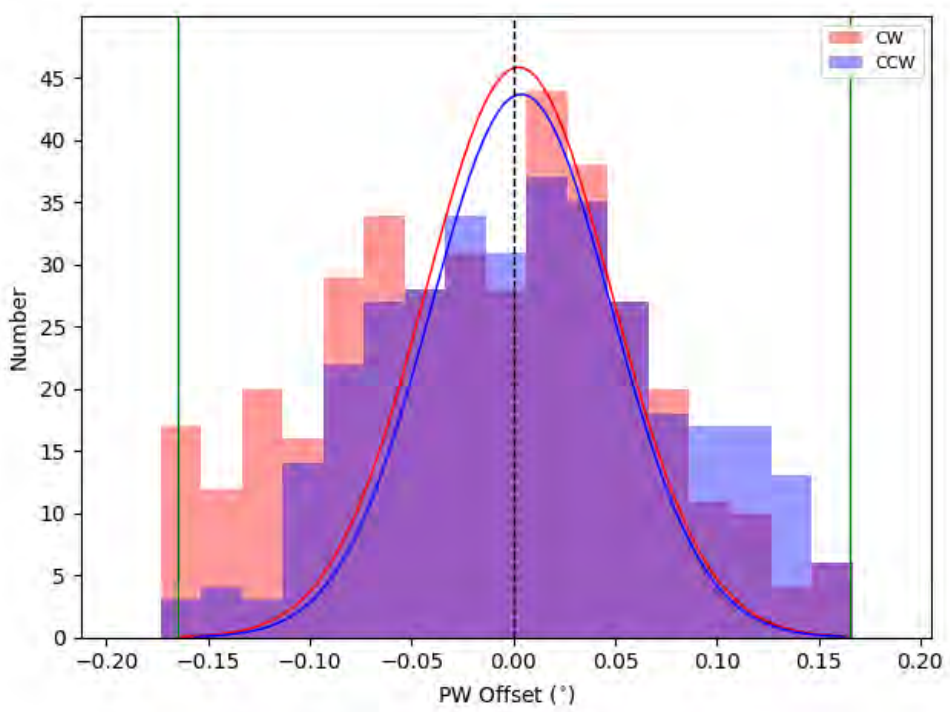

Figure 4-2. The combined offsets between the observed wheel position and the expected center position in wheel degrees are plotted for all the PW elements. The vertical dashed and green lines are as in Fig. 4-1. The solid lines represent fits of the normal distribution to the core of the CW and CCW distributions (within a half motor step).

In Fig. 4-3, the offsets of Fig. 4-2 are plotted on their date of observation. The denser vertical lines are due to large programs that make extensive use of the DW. For example, the Cycle 1 calibration program APT 1510 WFSS Wavelength Calibration was executed on Jul 9, 2022 and it uses the six blocking filters in the PW and the GR150C, GR150R, and CLEAR elements in the FW repeatedly. By visual inspection, we easily notice the excess of CW (red dots) and CCW (blue dots) data points at the bottom and top of the figure, respectively.

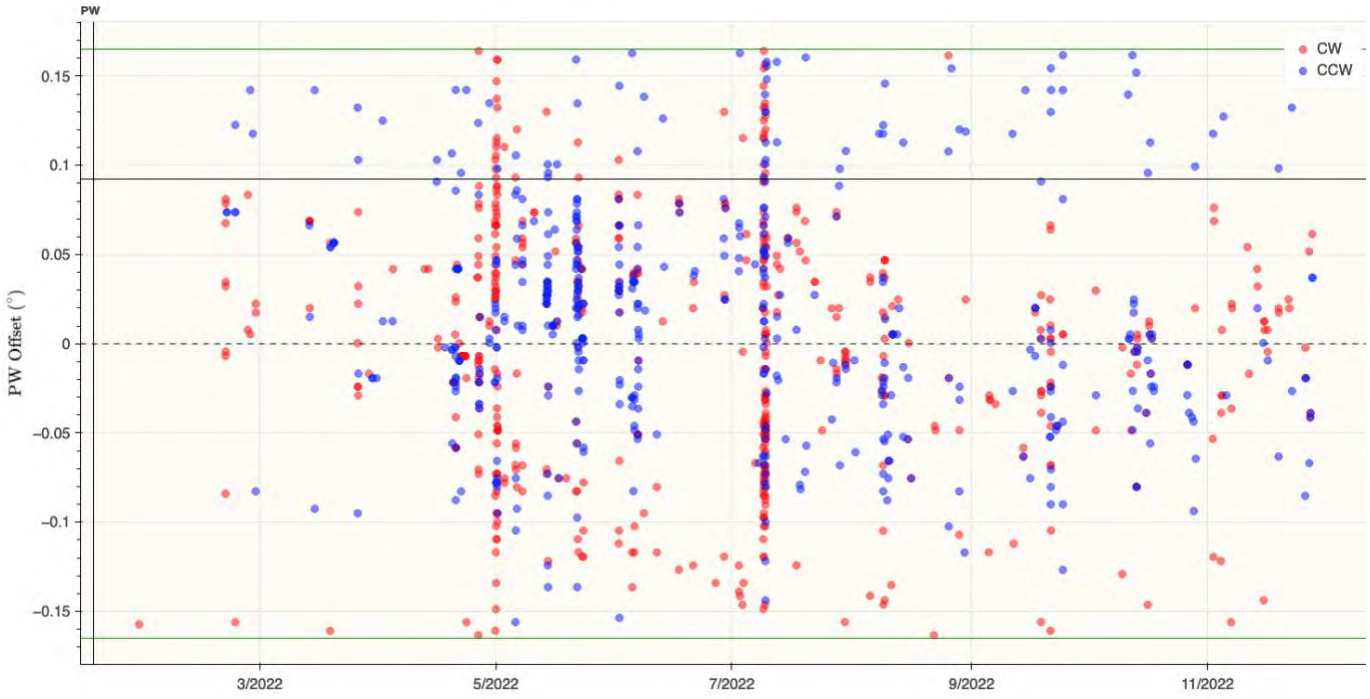

Figure 4-3. The offsets of Fig. 4-2 are plotted on their date of observation. The dense vertical lines are produced by large NIRISS programs that involved numerous steps of the PW.

4.2.2 Filter Wheel

As for the wheel positions and offsets of the PW, we show the equivalent figures for the FW in Figs. 4-4 to 4-6. The bimodality of the offsets is significantly more pronounced than for the PW. For example, in Fig. 4-4, we immediately notice that the elements settle near their expected position (vertical dashed line) but also at lower values for CW motions (red), e.g., CLEAR, F380M, F430M, F480M, and GR150R, and at higher values for CCW motions (blue), e.g., F380M, GR150C, and GR150R. But all the positions are within the range of ± 1 motor step (green vertical solid lines). This behavior is more apparent when plotting the offsets of the observed positions of all the elements from their expected positions (Fig. 4-5). For CW motions (red), the distribution is heavily skewed to negative offsets and the FW settles in either the primary, broad peak around $0.03°$ or a secondary, narrow peak around $-0.13°$. The trend is reversed for the CCW motions (blue). The primary, broad peak is centered around $0.00°$ while the secondary, narrow peak is at a positive offset around $0.12°$. In Fig. 4-6, the offsets are plotted as a function of the date of observation. Clearly, the negative offsets of the CW motions (red dots) dominate the lower part of the figure while the positive offsets of the CCW motions (blue dots) dominate the upper part.

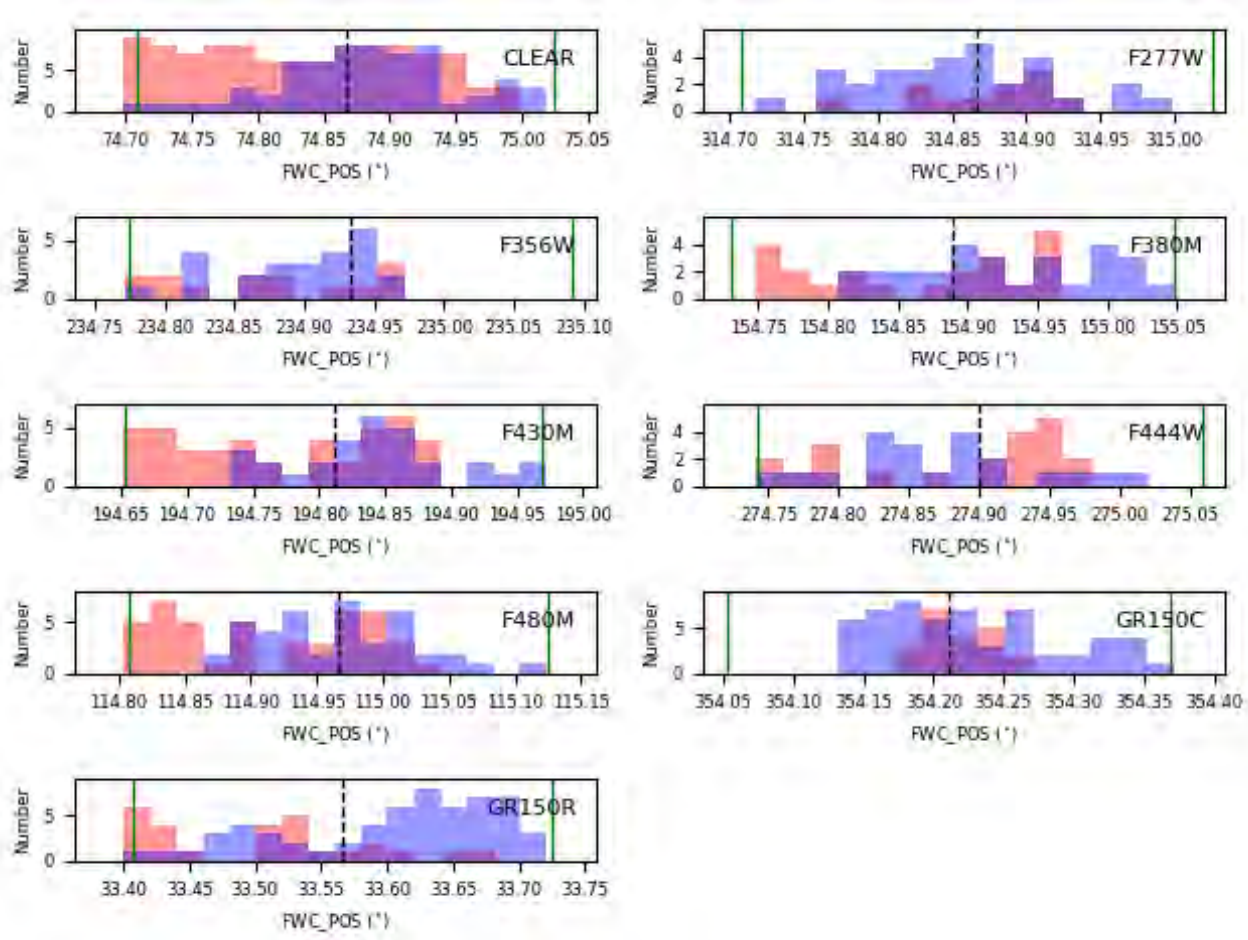

Figure 4-4. The distribution of the observed position of each FW element in wheel degrees (FWC_POS) is shown. The vertical dashed line denotes the expected center position and the green lines the uncertainty of one motor step ($\pm 0.1585°$). The CW rotations are in red and CCW in blue.

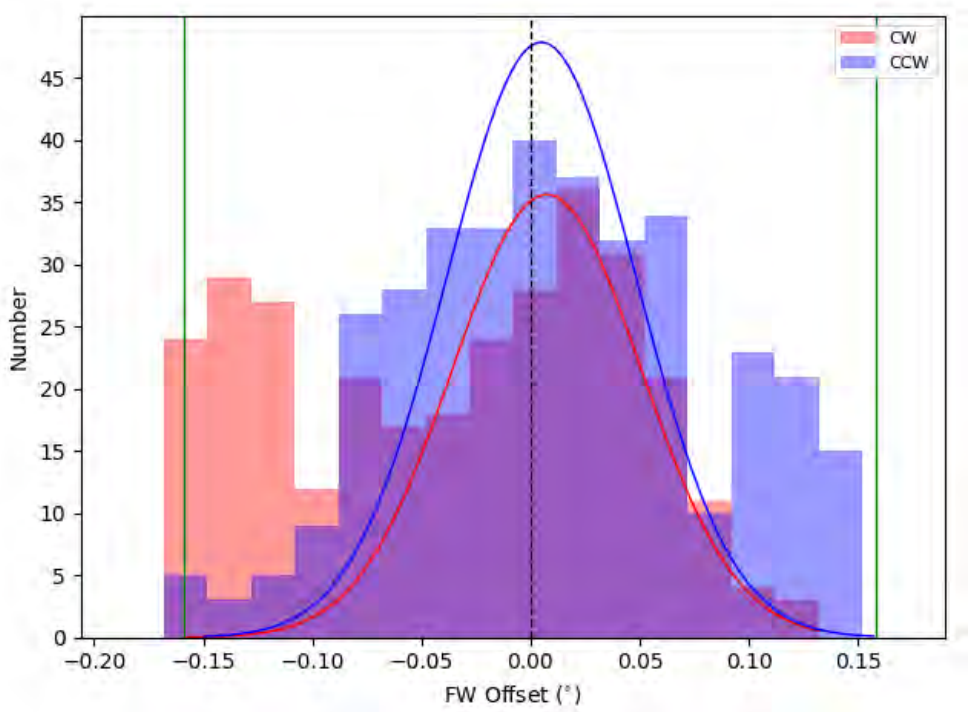

Figure 4-5. The combined offsets between the observed wheel position and the expected center position in wheel degrees are plotted for all the FW elements. The vertical dashed and green lines are as in Fig. 4-4. The solid lines represent fits of the normal distribution to the core of the CW and CCW distributions (within a half motor step).

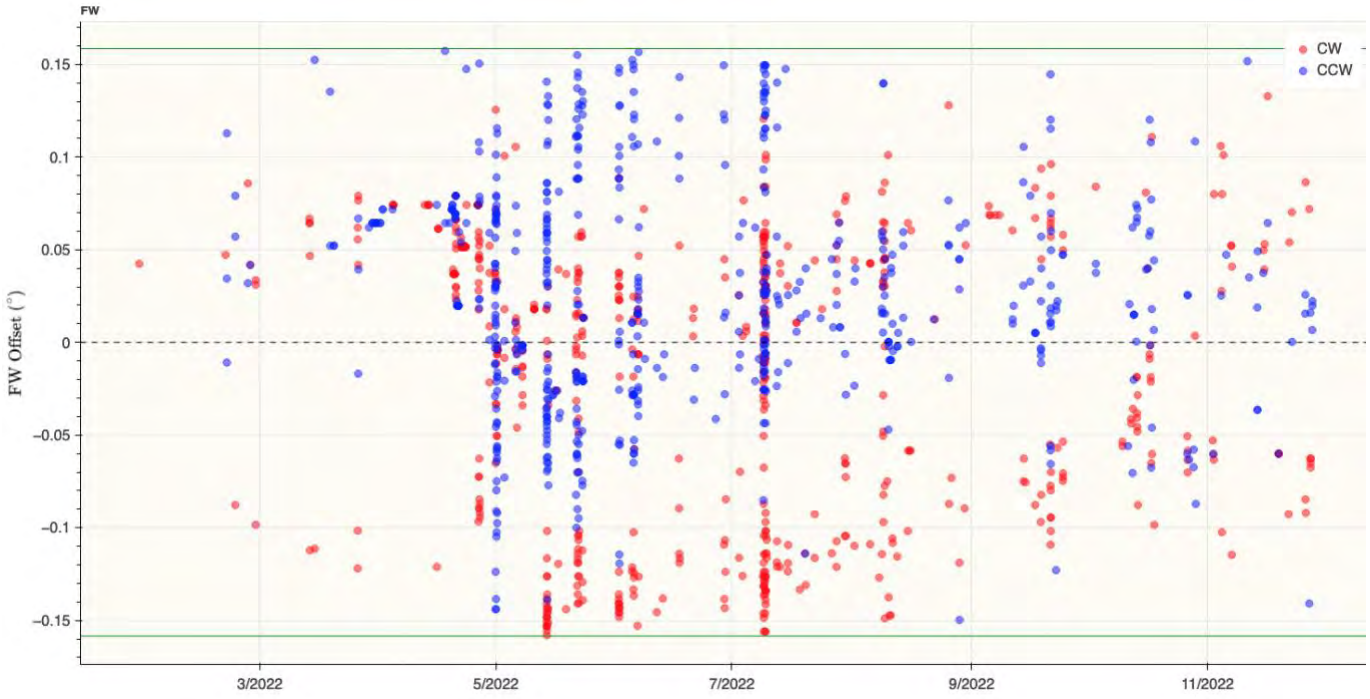

Figure 4-6. The offsets of Fig. 4-5 are plotted on their date of observation. The dense vertical lines are produced by large NIRISS programs that involved numerous steps of the FW.

4.3 Consecutive Exposures

Here, we take a closer look at the behavior of the wheels in consecutive exposures in the same wheel element. At the beginning of every exposure, the OSS script always sends a command to set up the wheel to the requested wheel element. The wheel driver is turned on to verify the current location, INIS_PWC_MDSTAT = MTR_OFF_DRVR_ON. If the wheel is not at the expected location, the motor is turned on and the wheel is moved, INIS_PWC_MDSTAT = MTR_AND_DRVR_ON and MTR_MOVING. The FSW minimizes the number of steps to rotate from one element to another and since there are nine elements per wheel, the number of steps can therefore vary from 1 to 4.

In the case of consecutive exposures in the same wheel element, we find that the position of the element can remain the same or can change slightly. For example, we show a series of exposures in the F158M filter in Fig. 4-7 collected as part of NIS-006 Darks (APT 1081) on Apr 21, 2022. At the beginning of each exposure, INIS_PWC_MDSTAT = MTR_OFF_DRVR_ON and the wheel remains at a constant position of INIS_PWC_POS = 44.97933° throughout all the exposures. But there are some exceptions as illustrated in Fig. 4-8. Consecutive exposures in F150W were taken as part of NIS-015 GR150C/R Flux Calibration (APT 1089) on May 22, 2022. Again, at the beginning of each exposure, INIS_PWC_MDSTAT = MTR_OFF_DRVR_ON but the position of F150W moves slightly between the exposures, i.e., 124.9476°, 124.9500°, 124.9548°, and 124.9572°. The wheel motor was not activated for these small moves. Surprisingly, in this particular case, the positions do not iterate towards the expected position of 124.9032° but diverge away from it. We note that these PW positions are correctly logged in the FITS header keyword PWCPOS.

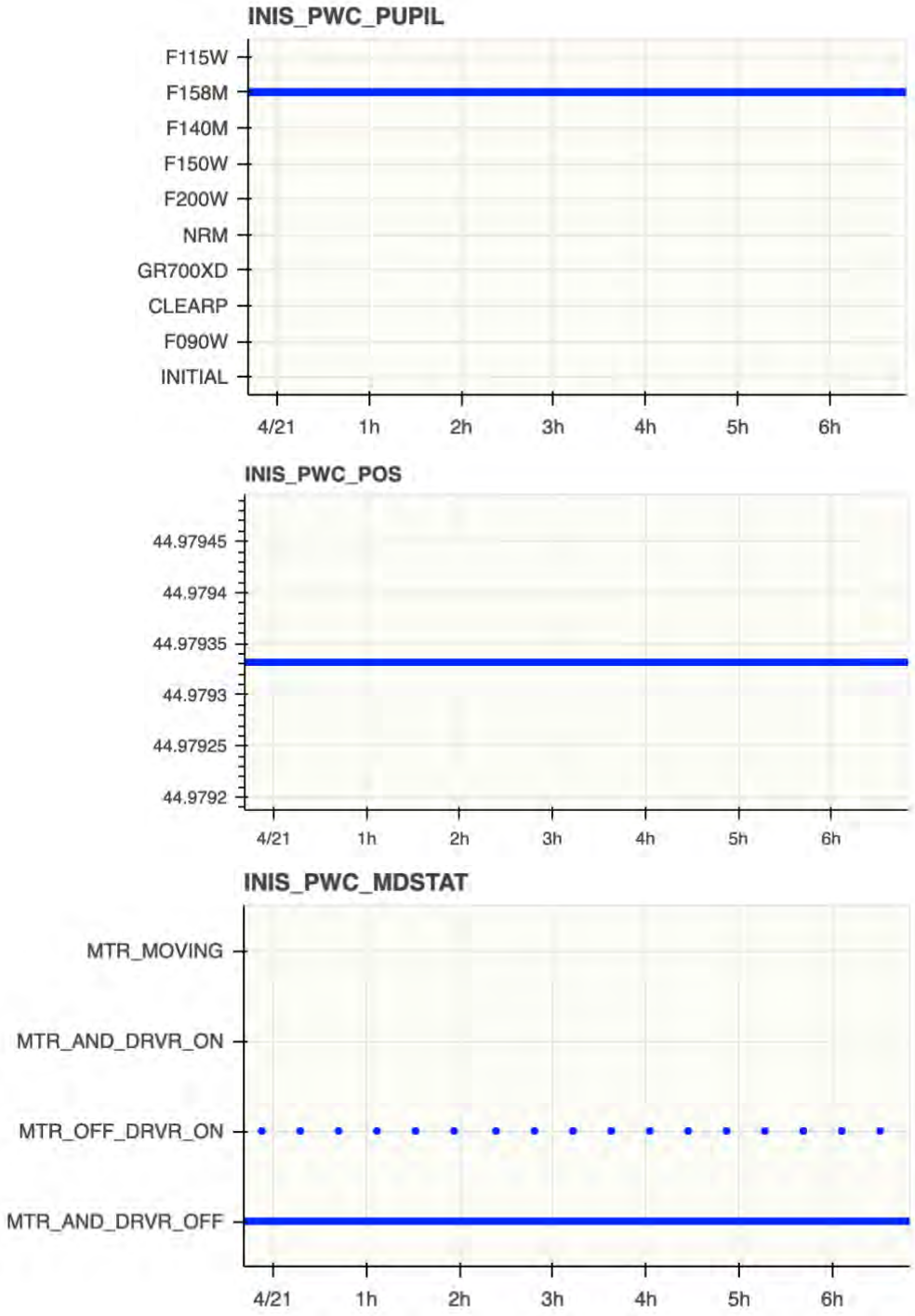

Figure 4-7. The F158M position and the state of the motor and driver are shown for a series of darks from program NIS-006 Darks (APT 1081) on Apr 21, 2022.

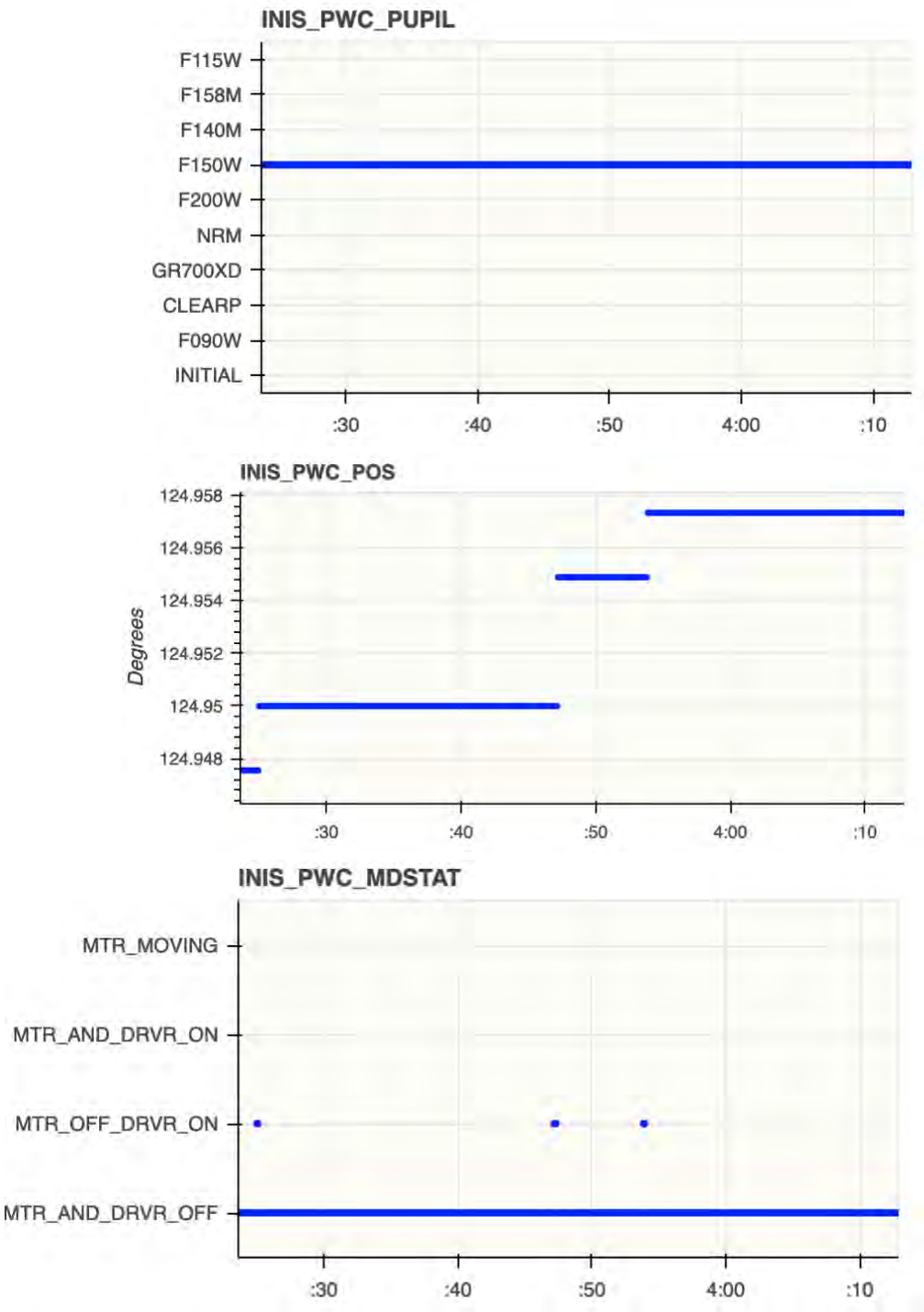

Figure 4-8. The F150W position and the state of the motor and driver are shown for a series of exposures from program NIS-015 GR150C/R Flux Calibration (APT 1089) on May 22, 2022.

To further characterize the behavior of the wheels when consecutive exposures are collected in the same wheel element, we plot the wheel offsets as a function of the exposure number in Figs. 4-9 and 4-10 for the PW and FW, respectively. Only sequences of exposures that show a wheel movement are considered. We find that for some elements, such as CLEARP, F150W, F200W, GR700XD, NRM, CLEAR, F277W, F430M, F444W, and F480M, the offsets show less "spread" in the second exposure than in the first exposure. This is apparent from the standard deviations of the offsets for the first and second exposures tabulated in Table 4-3. For the PW, the standard deviation decreases from 0.086° to 0.059° and for the FW, from 0.083° to 0.045°. The smaller spread in the second exposure suggests that the positions are likely converging to the commanded positions (horizontal dashed line at 0° in the offsets). Although sequences of three consecutive exposures or more are far fewer, we find that the offsets in the third exposure show a similar spread as for the second exposure.

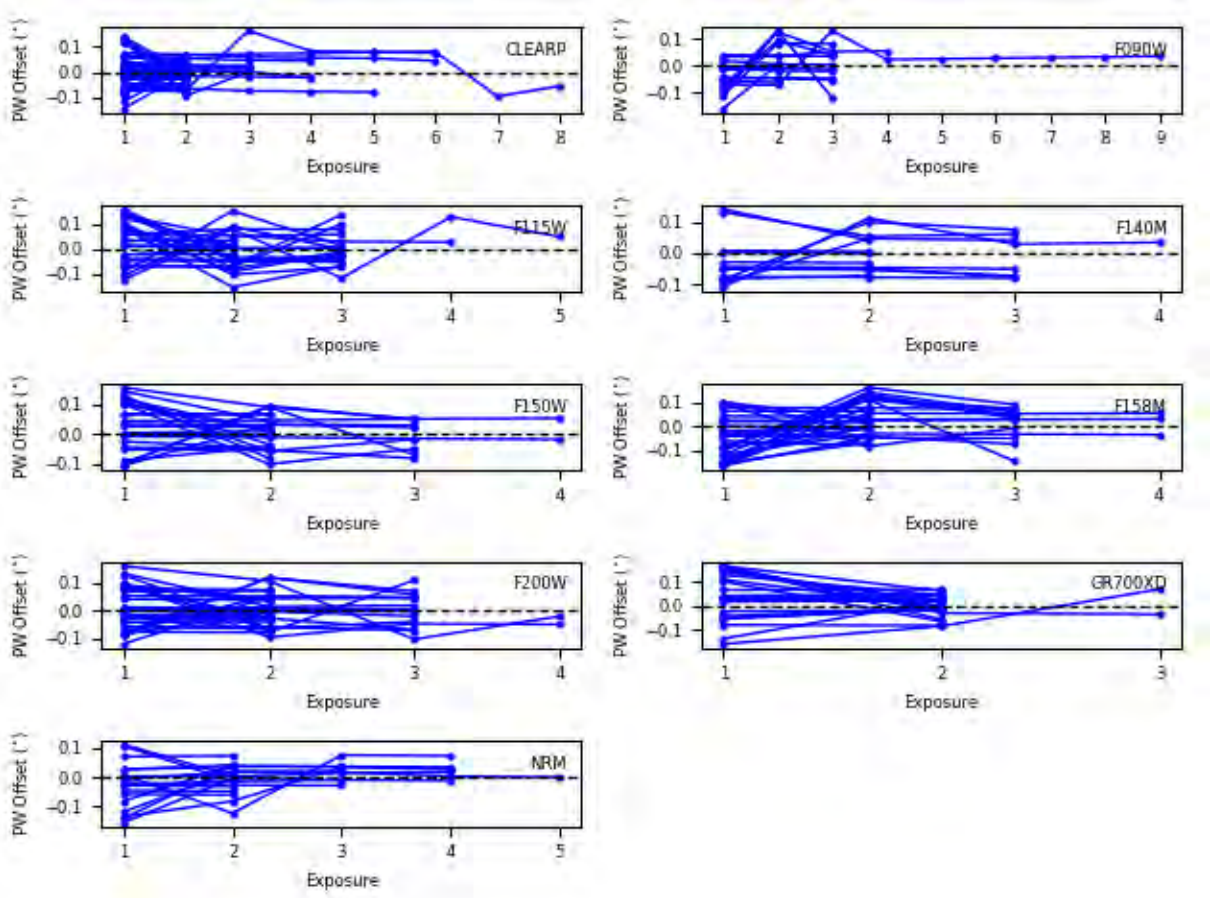

Figure 4-9. For each PW element, the offsets between the observed wheel position and the expected center position are plotted for a series of consecutive exposures.

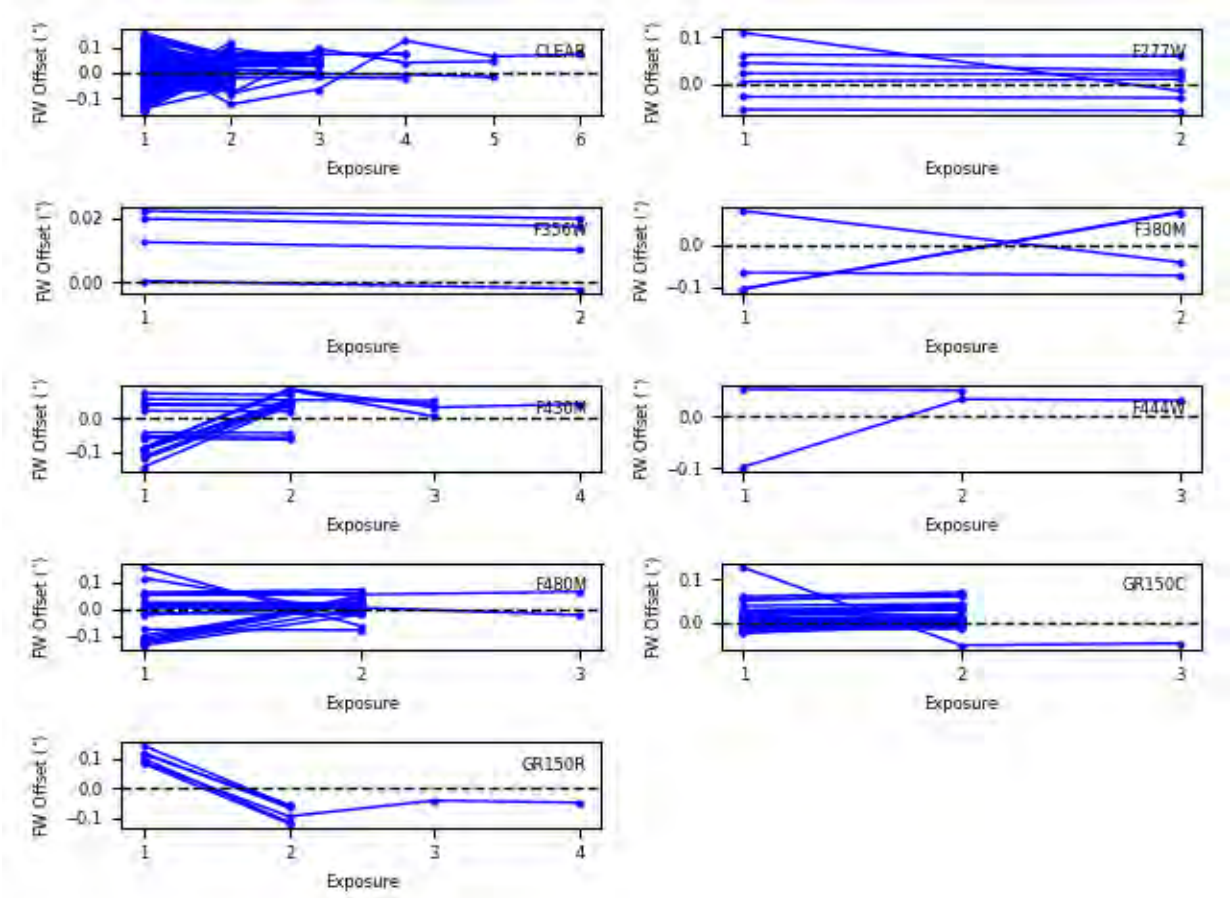

Figure 4-10. For each FW element, the offsets between the observed wheel position and the expected center position are plotted for a series of consecutive exposures.

Table 4-3. Offsets in Consecutive Exposures

Exposure	PW Offsets (°)	FW Offsets (°)
1	0.000 ± 0.085	-0.022 ± 0.083
2	0.004 ± 0.058	0.020 ± 0.045
3	0.008 ± 0.058	0.028 ± 0.040

4.4 VR Voltages

The voltages of the VR sensor are plotted in Figs. 4-11 and 4-12 for the PW and FW, respectively. The voltage is high (red) when position 1 (F090W for the PW and GR150R for the FW) is in the light path and low (blue) when any other wheel element is active. For both wheels, there is a small but noticeable downward trend in the voltages throughout the cooldown. The voltages stabilize on Apr 15, 2022 when NIRISS officially reached its cold plateau and its FPA heater was activated for the first time in orbit. The mean and standard deviation of the voltages at the cold plateau in the different states are given in Table 4-4. The values are as expected and appear stable over this period. The slight differences from the OTIS campaign voltages are expected because of the different ground cryo and on-orbit environments.

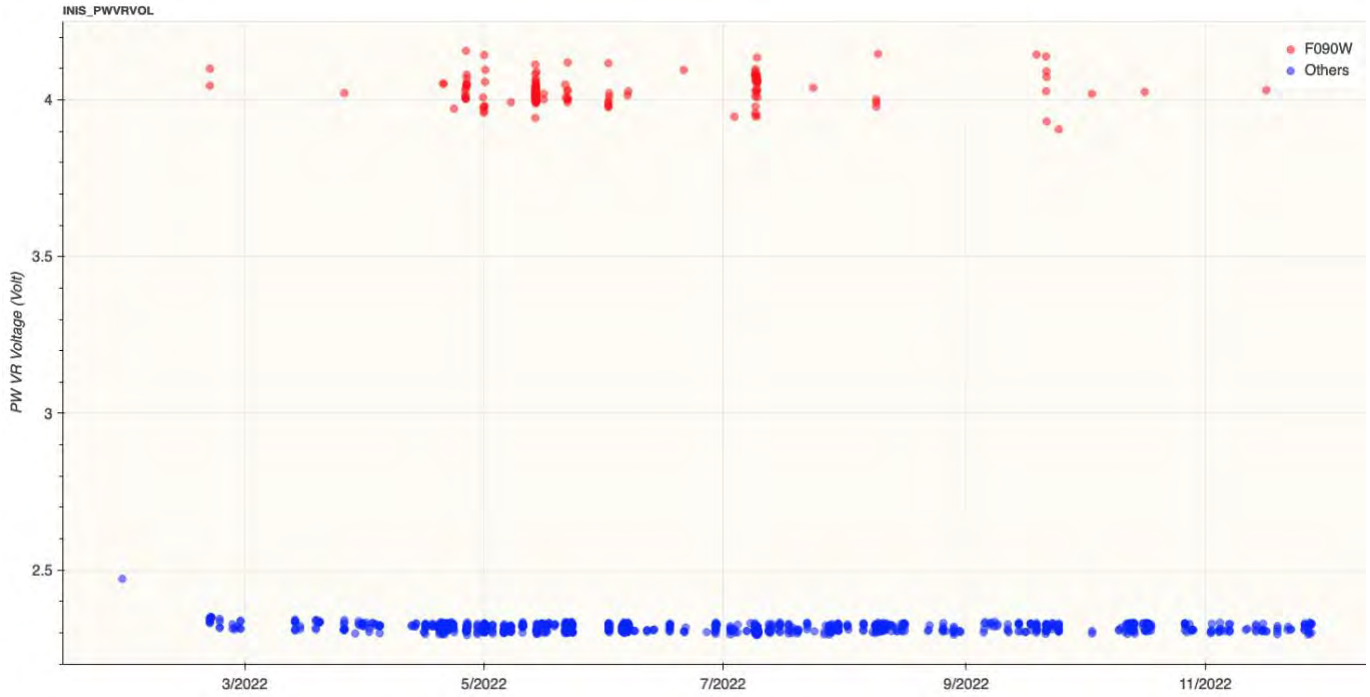

Figure 4-11. The voltage of the PW VR sensor is plotted since NIRISS was powered on. Position 1 (F090W) is in red and the other PW positions are in blue.

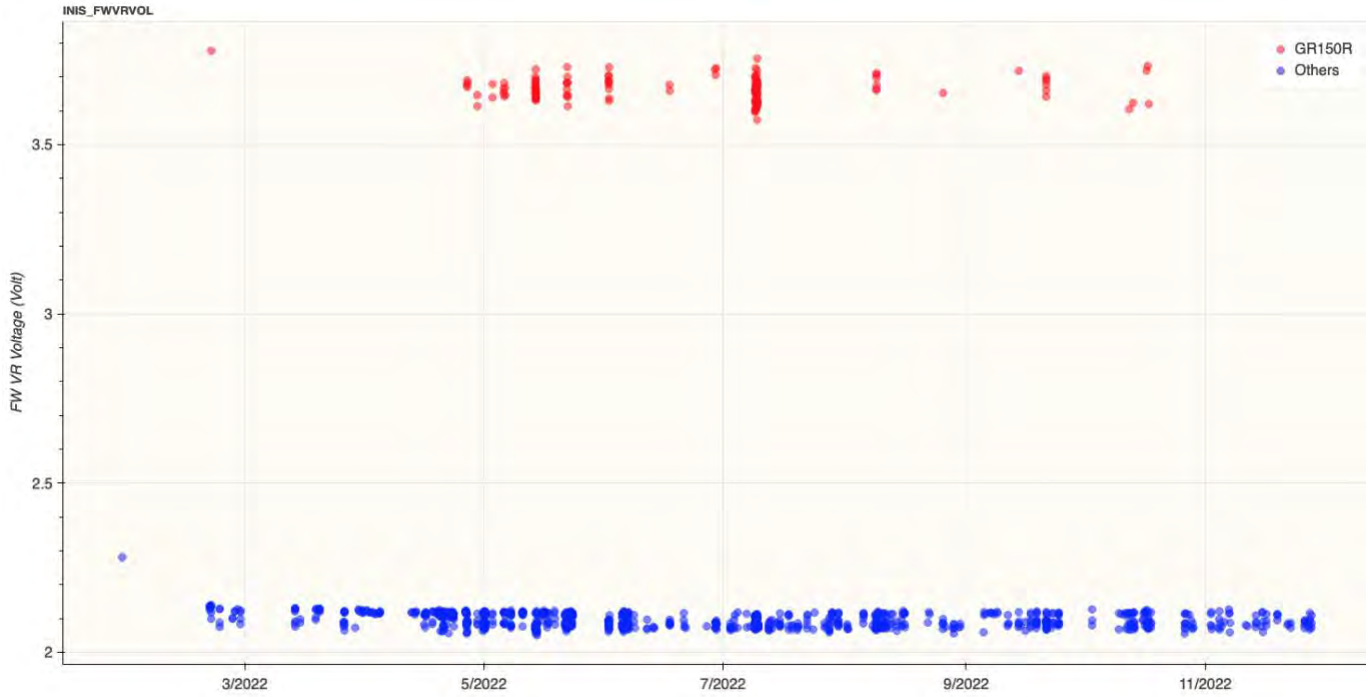

Figure 4-12. The voltage of the FW VR sensor is plotted since NIRISS was powered on. Position 1 (GR150R) is in red and the other FW positions are in blue.

Table 4-4. VR Sensor Voltages

Mnemonic	Value (Volt)
INIS_PWVRVOL	Position 1 (F090W): 4.03 ± 0.04
	Other positions: 2.32 ± 0.01
INIS_FWVRVOL	Position 1 (GR150R): 3.66 ± 0.04
	Other positions: 2.10 ± 0.02

5 Conclusion

The health and performance of the PW and FW of NIRISS were successfully verified for the ten months following the power-on and initialization of the instrument. The absolute positions of all the elements of both wheels settle within their expected range of ± 1 motor steps. For the FW, the distribution of the positions is bimodal with a primary peak around the expected center positions and a secondary peak offset by about $-0.13°$ for a CW motion and $0.12°$ for a CCW motion of the wheel. The distribution of the PW positions is mostly skewed towards negative offsets for a CW motion. In some sequences of consecutive exposures in the same wheel element, the wheel unexpectedly moves between the exposures. The cause of this behavior is unknown. The voltages of the VR sensor at position 1 (F090W for the PW and GR150R for the FW) and at all other positions are as expected and are stable for both wheels at the cold operating temperature. These on-orbit results are generally consistent with those of the CV3 cryo campaign presented in Martel (2016) but should now supersede them.

The current behavior of the DW is nominal and has no deleterious impact on the science observations. For the three grisms of the SOSS and WFSS modes, consecutive exposures might show slight differences in the tilt of the spectra. The spectral extraction software of these two modes is able to cope with these cases to create well calibrated, final combined spectra.

6 References

Delamer et al. 2015, JWST FGS PFM Limited Life Mechanism Operation, TNO/CSA/51274/1004, Rev. P0

Martel, A.R. 2016, Analysis of NIRISS CV3 Data: The Repeatability of the PW and the FW, JWST-STScI-004964 (Baltimore: STScI)

Martel, A.R. 2020, Analysis of NIRISS OTIS Data: The Repeatability of the PW and FW, JWST-STScI-006035 (Baltimore: STScI)

Martel, A.R. 2021a, NAP-004: NIS-004 NIRISS PW Calibration (NGAS CAR-343, APT 1079), JWST-STScI-007694 (Baltimore: STScI)

Martel, A.R. 2021b, NAP-005: NIS-005 NIRISS FW Calibration (NGAS CAR-344, APT 1080), JWST-STScI-007695 (Baltimore: STScI)

Martel, A.R. and the NIRISS Team 2022, The Commissioning of JWST NIRISS, JWST-STScI-008232 (Baltimore: STScI)

Vila Costas, M.B. 2015, FGS/NIRISS Limited Life Items (LLI) Usage and Allocation Planner, JWST-REF-023750 Rev –